Article

[handwritten: David Goodsell 2018 (Membrane is fluid)] [handwritten: vasicular endo & exocytosis (In.) (Exa)]

Local Dendritic Activity Sets Release Probability at Hippocampal Synapses

Tiago Branco,[1,2,*] Kevin Staras,[1,3] Kevin J. Darcy,[1] and Yukiko Goda[1,2,*]
[1]MRC Laboratory for Molecular Cell Biology and Cell Biology Unit
[2]Department of Neuroscience, Physiology and Pharmacology
University College London, Gower Street, London WC1E 6BT, UK
[3]Present address: School of Life Sciences, University of Sussex, Brighton BN1 9QG, UK
*Correspondence: t.branco@ucl.ac.uk (T.B.), y.goda@ucl.ac.uk (Y.G.)
DOI 10.1016/j.neuron.2008.07.006

[handwritten: connectomics. — 1 nm resolution]

SUMMARY

The arrival of an action potential at a synapse triggers neurotransmitter release with a limited probability, p_r. Although p_r is a fundamental parameter in defining synaptic efficacy, it is not uniform across all synapses, and the mechanisms by which a given synapse sets its basal release probability are unknown. By measuring p_r at single presynaptic terminals in connected pairs of hippocampal neurons, we show that neighboring synapses on the same dendritic branch have very similar release probabilities, and p_r is negatively correlated with the number of synapses on the branch. Increasing dendritic depolarization elicits a homeostatic decrease in p_r, and equalizing activity in the dendrite significantly reduces its variability. Our results indicate that local dendritic activity is the major determinant of basal release probability, and we suggest that this feedback regulation might be required to maintain synapses in their operational range.

INTRODUCTION

Release probability (p_r) is the likelihood of vesicle fusion and transmitter release occurring at a presynaptic terminal in response to an action potential (Del Castillo and Katz, 1954). This fundamental parameter is critical in determining the strength of a synapse as well as its dynamic adaptation to input, and, as such, it shapes the nature of neuron-neuron communication (Maass and Zador, 1999). Studies from a variety of systems indicate that release probability at individual synapses is unique (Atwood and Bittner, 1971; Frank, 1973; Cooper et al., 1996; Dobrunz and Stevens, 1997). However, the factors contributing to the setting of p_r at each synaptic terminal still remain to be determined. Extensive experimental evidence from work on neuromuscular junction and invertebrate and vertebrate central synapses has suggested that release probability along single axons depends on the identity of the postsynaptic target (Bennett et al., 1986; Robitaille and Tremblay, 1987; Katz et al., 1993; Muller and Nicholls, 1974; Koerber and Mendell, 1991; Mennerick and Zorumski, 1995; Davis, 1995; Reyes et al.,

[handwritten: FM dye based imaging]

1998; Koester and Johnston, 2005). However, this simple relationship is not universal; for example, inputs on the same target can exhibit considerable variability (Jack et al., 1981; Redman and Walmsley, 1983; Walmsley et al., 1988; Redman, 1990; Hessler et al., 1993; Dobrunz and Stevens, 1997; Huang and Stevens, 1997), and in the limiting case of autaptic cell cultures, release probability can be highly nonuniform (Rosenmund et al., 1993; Murthy et al., 1997; Slutsky et al., 2004; Granseth et al., 2006). Thus, ==release sites from a single axon can have variable p_r, even when making contact on the same postsynaptic neuron.== Aside from signaling mechanisms specific to the identity of the postsynaptic cell, there must be other factors contributing to the setting of release probability. At present, it is not known what these factors might be. Moreover, the potential functional relevance of p_r nonuniformity in the connection between two cells remains to be established.

In the present study, we combine the use of simple networks of dissociated hippocampal cultured neurons with fluorescence imaging, electrophysiological recordings, and ultrastructural analysis to establish the cellular principles used by synapses to define their basal release probability. We find that, despite high overall variability, synapses from single axons contacting one dendritic tree have highly correlated release probabilities when they converge on the same branch of the dendrite. Furthermore, p_r homeostatically adapts both to the number of synapses in the branch and to selective increases in postsynaptic activity. This organization of p_r can be disrupted not only by global but also by local activity manipulations. Our findings suggest that p_r is set according to the local level of dendritic depolarization.

RESULTS

Release Probability Is Dendritically Segregated

Using sparse cultured networks that permit a detailed characterization of individual synapses in an identified connection, we first examined p_r across the dendritic trees of single neurons. Cells were filled with Alexa dyes, and synaptic contact points were identified using FM4-64. To measure p_r at individual synapses, we evoked synaptic activity with field stimulation and imaged fluorescence loss due to vesicle exocytosis from the FM-dye-labeled synapses, where the rate of fluorescence decay is proportional to p_r (Zakharenko et al., 2001) (Figure S1 available online). Consistent with previous reports (Murthy et al., 1997; Slutsky et al., 2004), p_r had a broad and skewed distribution
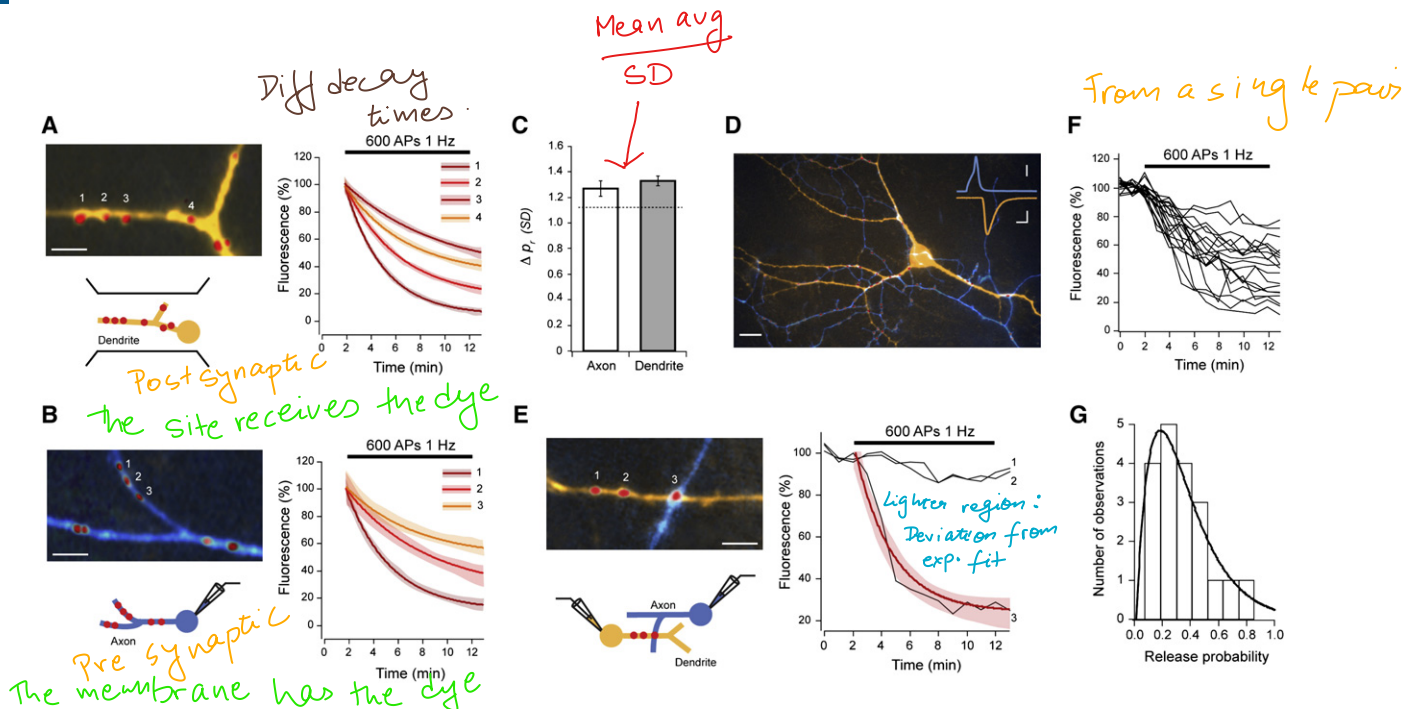
Figure 1. Variability of Release Probability

Release probability was measured by labeling synapses with FM dye and monitoring destaining rates upon action potential stimulation, delivered by field stimulation (A) or during single (B) and paired (E) whole-cell recordings.

(A) (Left) Dendrite (orange) with FM4-64-labeled synapses (red). (Right) Destaining curve fits with 95% confidence interval (shaded areas) for the numbered synapses show a wide range of release probabilities for synapses in the same dendritic branch. Scale bar, 5 μm.

(B) (Left) Axon (blue) with several synapses (red) and respective destaining curve fits (right) also show very different p_rs for synapses along single axons. Scale bar, 5 μm.

(C) Summary data of similarity comparisons for all synapses in a branch of dendrite or axon, showing that the mean p_r difference is not significantly different from the average p_r difference expected by chance (1.13 SDs, Wilcoxon rank sum test for axon p = 0.4241, dendrite p = 0.2079).

(D) Epifluorescence image of axon (blue) making multiple synaptic contacts (red, FM4-64) with a postsynaptic cell (orange). (Inset) Representative traces of AP (blue) and evoked EPSC (orange). Scale bars, 15 μm; inset, 2 ms, 20 mV (top), 100 pA (bottom).

(E) Stimulation of the presynaptic cell selectively destains FM4-64 fluorescence from the synapse belonging to the labeled axon (3) and not from those originating from unlabeled axons (1 and 2). Red line is a single exponential fit. Scale bar, 5 μm.

(F and G) Destaining traces from 19 synapses from one connection (F) and corresponding release probability frequency histogram (G). Solid line is γ function fit (λ = 5.8, n = 3).

Error bars are ± SEM.

with an average median of 0.22 ± 0.03 and mean coefficient of variation (CV) of 0.66 ± 0.06 (n = 12 cells). To address what underlies this high variability of release probabilities, we then carried out a detailed analysis of p_r distribution. To do this, we first computed the absolute p_r difference between each synapse in a given cell and all other synapses from the same cell. This yielded a mean absolute p_r difference of 0.19 ± 0.03, a value that was similar to that expected by random sampling of the measured p_r distribution (0.18, p = 0.8116). We next normalized p_r differences for each synapse pair by the standard deviation of each cell to generate a measure that allowed us to quantify the magnitude of the similarity between any two synapses in a given cell. This gave a mean difference of 1.27 ± 0.20 SDs for all cells analyzed. Using this measure, we then analyzed the spatial distribution of p_r along the dendrites by computing the average p_r difference between all synapses on single dendritic branches. We found that even for single branches there was a large variability in release probability (mean difference = 1.33 ± 0.04 SDs, not different from global mean difference, p = 0.4449; CV = 0.61 ± 0.06, not different from global CV, p = 0.5576; Figures 1A and 1C). This finding is in accordance with previous ultrastructural data from native hippocampal tissue where the size of presynap-

tic terminals onto dendritic branches is highly nonuniform (Harris and Sultan, 1995). Next, using whole-cell patch clamp, we stimulated target neurons and measured p_r at all synapses on the axonal arbor of single cells. Again, we found a large variability for synapses in individual axonal branches (mean difference = 1.27 ± 0.06 SDs, not different from global mean difference, p = 0.4792; CV = 0.69 ± 0.09, not different from global CV, p = 0.7945, n = 5 cells; Figures 1B and 1C). Furthermore, no relationship was found between p_r and distance to the soma along the dendrite or the axon (Figure S2A). Interestingly, a small but significant negative correlation was found between synaptic density and release probability of synapses along a dendrite (R = −0.38, p = 0.0351; Figure S2B), although no such relationship was found for synapses along the axon.

To remove the potential sources of variability on p_r arising from examining a mixed population of synapses with different neuronal sources or targets, we next restricted our analysis to synapses connecting two neurons. Excitatory postsynaptic currents (EPSCs) were recorded with paired whole-cell patch clamp, and synaptic contact points were identified using FM4-64 and Alexa dye fills of axons and dendrites (Figures 1D and 1E). On average, we detected 8 ± 5.4 (SD) contact points between two

Neuro-muscular synapses have high Pr.

Neuron

Local Dendritic Regulation of Release Probability

No relation b/w Pr and distance of synapse from cell soma. In hippocampus, variability is ↑, but Pr seems to be low.

same (axon, cell), high variation

same (axon, dend), Pr has low variance

If you have multiple connecti b/w (A&D), release is distributed among synapse
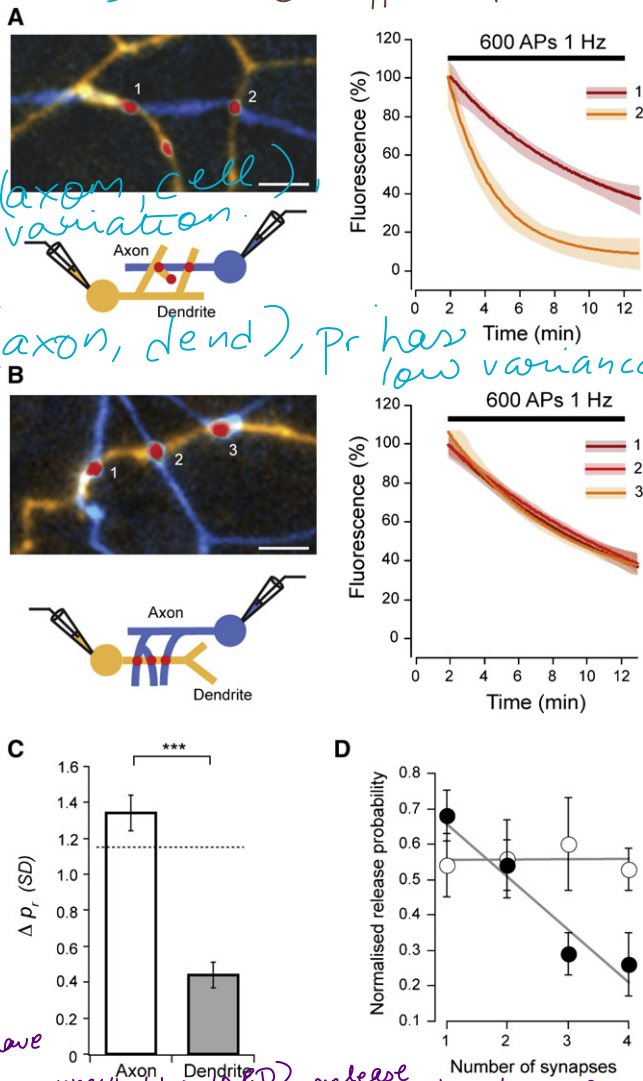
Figure 2. Release Probability Is Dendritically Segregated
(A and B) Images (left) and destaining curve fits (right) for synaptic contacts between a cell pair, on different (A) or the same dendritic branches (B) of the postsynaptic neuron (axon is blue and dendrite is orange). Release probability of synapses on the same dendritic branch is very similar. Scale bars, 5 μm.
(C) Summary of similarity comparisons between synapse pairs. Dashed line indicates expected mean difference due to chance from Monte Carlo simulations (1.15 SDs, Wilcoxon rank sum test for axon p = 0.1023, dendrite p < 0.0001). Mean intersynaptic distances were not significantly different (axon versus dendrite, p = 0.1406, axon = 8.5 ± 5.3 μm [SD], dendrite = 5.9 ± 3.0 μm [SD]).
(D) Normalized release probability plotted against number of synapses in the axonal branch (open circles) and in the dendritic branch (closed circles). p_r homeostatically adapts to the number of synapses made by the presynaptic cell onto the same dendritic branch. Lines are linear fits to the data. Error bars are ± SEM.

cells with the culture conditions used. This is comparable to findings in intact tissue, where multiple synapses have been found with light microscopy and ultrastructural analysis in connections between stratum radiatum-CA1 pyramids (Sorra and Harris, 1993) and CA1 and CA3 pyramidal cells-interneurons (Biró et al.,

2005; Wittner et al., 2006), and with quantal analysis in excitatory connections onto CA1 pyramids (Larkman et al., 1997). Even in this reduced synaptic population, p_r had a broad and skewed distribution with an average median of 0.22 ± 0.04 and mean CV of 0.51 ± 0.13 (n = 7 pairs, Figures 1F and 1G). The average absolute p_r difference between all synapses of a given connection was 0.19 ± 0.01, not different from the value expected by random sampling (0.17, p = 0.6383), corresponding to 1.29 ± 0.07 SDs. We then repeated the branch-specific spatial analysis as above for both axons and dendrites. We found that while p_r could be very different for synapses made along short segments of axons contacting different dendrites (mean difference = 1.34 ± 0.10 SDs, not different from global mean difference, p = 0.8652; CV = 0.48 ± 0.09, not different from global CV, p > 0.9999), p_r was very similar for synapses that shared the same dendritic branch (mean difference = 0.44 ± 0.07 SDs, significantly different from synapses made on different dendrites from the same axon, p < 0.0001, and from global mean difference, p < 0.0001; CV = 0.12 ± 0.04, significantly different from global CV, p = 0.0007; Figures 2A–2C). To confirm that p_r is segregated in a branch-specific manner, we analyzed release probability of synapses separated by dendritic branch points and found that in these cases p_r is markedly different (mean difference = 1.52 ± 0.26 SDs, p < 0.0001 compared with synapses made exclusively on the parent or daughter branch; Figure S3). We also analyzed recycling pool sizes and found that this parameter exhibited dendritic homogeneity similarly to p_r (Figure S4). Furthermore, release probability displayed a strong negative correlation with the number of synapses that the axon made on the dendritic branch (R = −0.53, p < 0.0001; Figure 2D), but not with the number of synapses along an axon contacting different dendrites (R = 0.01, p = 0.9349). These observations suggest that, for single inputs, p_r is not randomly distributed but rather that release probability is segregated at the level of individual dendrites.

Spatial Analysis of p_r at the Ultrastructural Level

We next examined the spatial distribution of p_r using ultrastructural analysis, where we could unequivocally identify single synapses and the axonal and dendritic processes they belong to at high resolution. To measure release probability, we directly counted the number of vesicles exocytosed in response to a defined number of action potentials (APs). This relied on FM1-43 photoconversion to distinguish vesicles labeled with FM dye after exo/endocytosis, which appear dark in electron micrographs, from nonlabeled vesicles (Harata et al., 2001; Schikorski and Stevens, 2001; Darcy et al., 2006). Synapses were FM1-43 loaded using field stimulation (30 APs, 1 Hz), identified at fluorescence level, and subsequently photoconverted, embedded, and serially sectioned (Figures 3A and 3C–3G). Labeled synapses (n = 31 from four cultures) had a median total pool size of 296 vesicles (interquartile range [IQR] = 306) and a median p_r of 0.37 (IQR = 0.75). Using this synapse population, we analyzed the spatial distribution of p_r by examining all cases where synapses (1) shared the same axon branch but different dendrite or (2) shared the same axon branch and same dendrite. Consistent with our fluorescence measurements, synapses made onto the same dendrite had very similar p_r (mean difference = 0.31 ± 0.14 SDs), while those contacting different dendrites had highly

[handwritten annotation at top: a) same axon, diff. dendrites b) same axon, same dendrite]
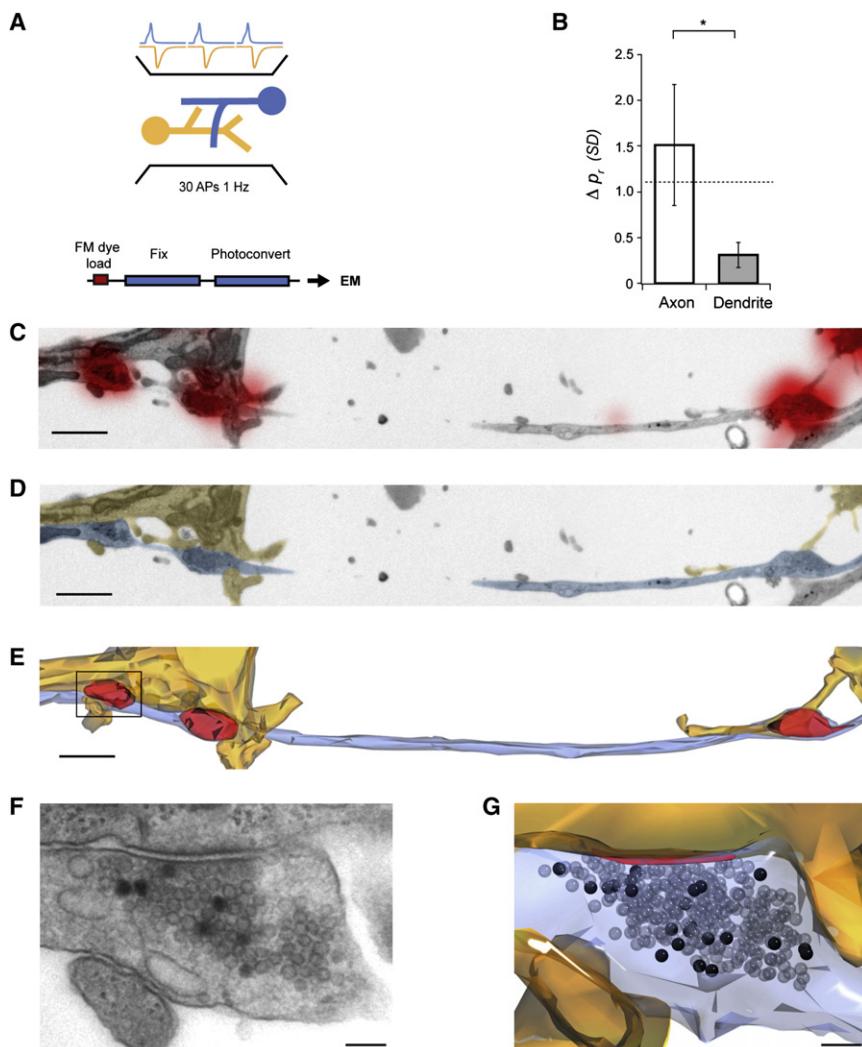

Figure 3. Ultrastructural Analysis of Release Probability

(A) Experimental scheme. FM dye was loaded into synapses with 30 APs delivered by field stimulation, and samples were photoconverted, serially sectioned, imaged, and reconstructed. Release probability was estimated by counting the number of photoconverted vesicles.

(B) Summary of similarity comparisons, showing that synapses on the same dendrite have very similar release probabilities (axon versus dendrite, p = 0.0438). Dashed line indicates the expected difference due to chance from Monte Carlo simulations (1.1 SDs, Wilcoxon rank sum test for axon p = 0.8750, dendrite p = 0.0156).

(C–E) Representative experiment showing one axon (blue) making synapses (red) with two different dendrites (orange). (C) Low-magnification electron micrograph with FM dye fluorescence overlaid. (D) Same micrograph as in (C) with axon and dendrite colored for clarity. (E) 3D reconstruction with vesicle clusters in red.

(F) Higher-magnification micrograph of the boxed synapse in (E) where photoconverted vesicles are clearly seen.

(G) 3D reconstruction of the same synapse with photoconverted vesicles (black) and active zone (red).

Scale bar in (C)–(E), 1 μm; (F) and (G), 100 nm. Error bars are ± SEM.

variable release probabilities (mean difference = 1.51 ± 0.66 SDs, p = 0.0438; Figure 3B).

P_r Responds Homeostatically to Increased Dendritic Activity

Taken together, our fluorescence and ultrastructural observations demonstrate that, in a connection between two neurons, neighboring synapses on the same dendritic segment have very similar release probabilities, whereas no such relationship is seen between p_r and the disposition of boutons along the axon. Moreover, p_r is negatively correlated with the number of synapses made by the axon onto the dendrite. These findings suggest that some form of dendritically coordinated homeostatic adaptation contributes to the local setting of basal release probability. We next sought to test this hypothesis by first establishing a condition that drives homeostatic changes in p_r and then examining the contribution of dendritic activity in altering p_r. We increased network activity by delivering APs at 1–2 Hz for 2 hr and estimated release probability with whole-cell paired recordings (Figure 4A). This manipulation resulted in a 23% ± 5% increase in the paired-pulse ratio (PPR) of EPSC amplitudes (control

PPR = 0.71 ± 0.05, n = 16), consistent with a decrease in release probability (t test, p = 0.0394, n = 8; Figure 4B). We next compared p_r between control and stimulated cultures using quantal analysis. EPSCs were recorded under low p_r conditions by adjusting the extracellular Ca^{2+}/Mg^{2+} ratio to the point where failures of evoked responses could be detected (control failure rate = 32% ± 3%, n = 7), which decreased the mean quantal content (control mean quantal content = 1.19 ± 0.09) and produced clearly quantized evoked responses (Figure 4C, right, inset) that, when converted to a frequency histogram, appeared as well-defined peaks. For each cell, we also recorded spontaneous miniature EPSCs and baseline noise, and an analysis of the histograms was performed as in Larkman et al. (1997). In all cells examined, clear, equally spaced peaks were identified, with the first and second peaks matching the baseline noise and mEPSC histograms, respectively (Figure 4C). We then fitted a compound binomial model to the identified peaks to extract mean release probability, number of active release sites (N), and p_r CV. Control values were p_r = 0.16 ± 0.04 (the reduced extracellular Ca^{2+}/Mg^{2+} compared to our FM dye experiments yields a lower p_r estimate), p_r CV = 0.50 ± 0.15 and N = 11 ± 0.5, in good agreement with the values obtained from FM dye destaining. Analysis of stimulated cultures showed a 70.0% ± 11% decrease in p_r (p = 0.0424, n = 4), with no change in N (p = 0.3420; Figure 4D). Therefore, release probability responds homeostatically to elevated network activity arising from the 2 hr stimulation protocol.
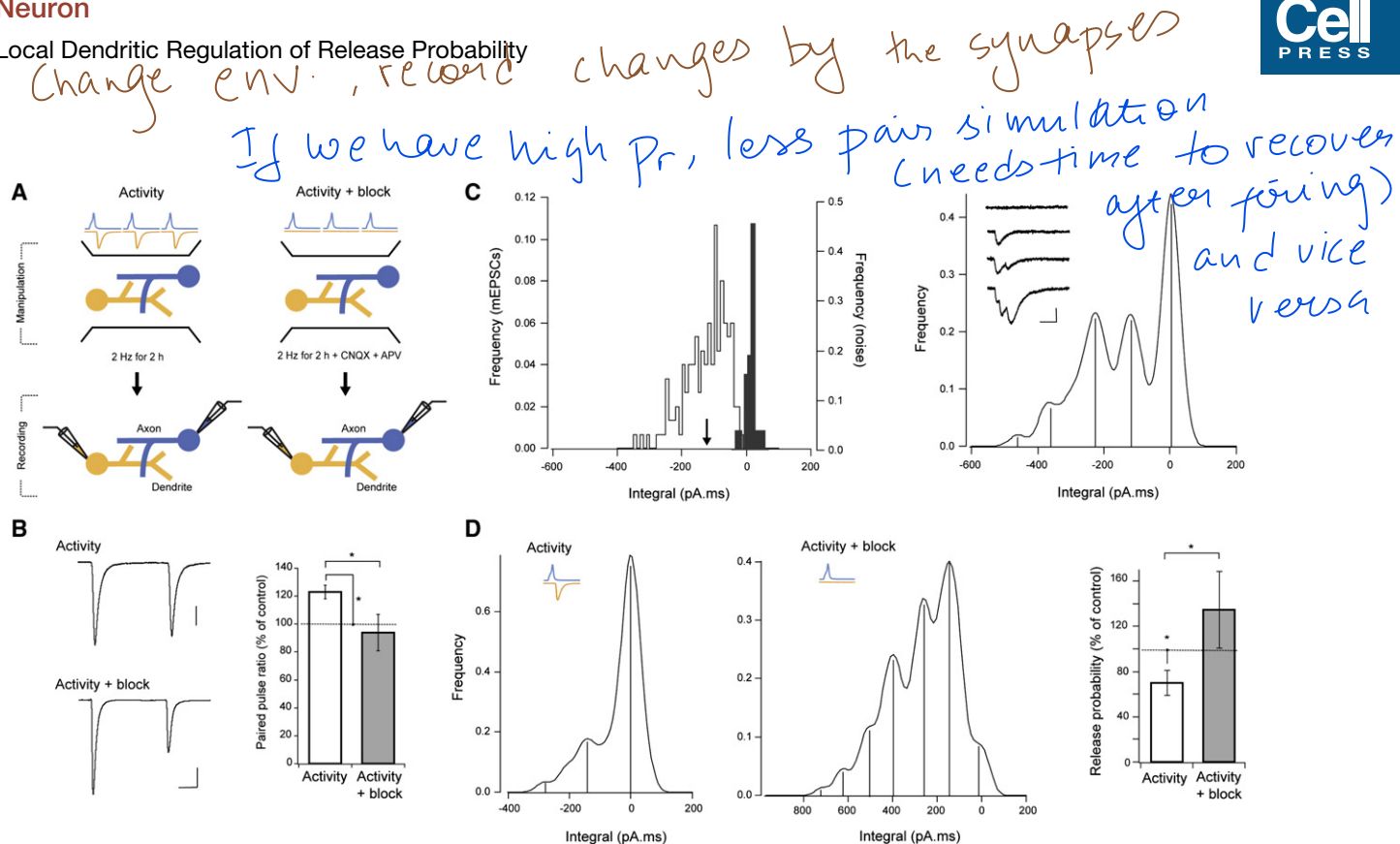
Figure 4. Release Probability Is Set by Dendritic Activity

(A) Two experimental schemes: activity (left) and activity + block (right). (Left) Activity in the culture was increased by delivering APs with field stimulation for 2 hr, and paired whole-cell recordings were used to assess the impact of this manipulation on release probability. (Right) For activity + block condition, a similar experimental scheme was used, but excitatory synaptic activity was blocked during stimulation.

(B) Example paired-pulse EPSC traces (left, averages of 20) and summary of paired-pulse EPSC amplitude ratio (right), showing an increase of PPR with activity, which is abolished by synaptic blockers. Scale bars, 15 ms, 200 pA top, 100 pA bottom.

(C and D) Recordings in 1 mM Ca^{2+}/3 mM Mg^{2+}. ([C], left) Frequency histogram of mEPSC integral (white) and baseline noise (gray). Arrowhead indicates the mEPSC integral mean. ([C], right) Smoothed histogram of evoked response integrals on the same postsynaptic cell, showing well-defined peaks at equally spaced distances. Note that the first two peaks correspond to the baseline noise and mEPSC mean in the left panel. Inset shows example traces where different number of quanta have been released. Scale bar, 2 ms, 50 pA. (D) Increasing activity leads to a significant decrease in release probability, which is abolished by blocking excitatory synaptic transmission. Smoothed integral histograms of evoked responses for example connections are shown, after increased activity alone (left), and with synaptic blockers (center). ([D], right) Summary of p_r changes for all connections. Error bars are ± SEM.

In order to determine whether homeostatic downregulation of p_r is specifically dependent on dendritic activity and how presynaptic activity might contribute to this process, we selectively silenced postsynaptic excitatory activity by stimulating the network in the presence of glutamate receptor blockers. We found no compelling evidence for neurotransmitter release modulation by presynaptic AMPA or NMDA receptors in our cultures (Figure S5), and thus this manipulation eliminates dendritic activity while allowing normal presynaptic function. Block of excitatory receptors significantly abolished the increase in PPR of evoked responses (t test, p = 0.0377, n = 6; Figure 4B). Moreover, quantal analysis (p = 0.0420, n = 4) revealed a tendency for release probability to be higher than in control, indicative of a homeostatic adaptation to reduced activity despite enhanced presynaptic stimulation (Figure 4D). As with the control activity alone condition, no changes were detected in the number of release sites. These results therefore strongly suggest that homeostatic adjustment of p_r depends on postsynaptic activation and that release of neurotransmitter from the presynaptic terminal by itself is not sufficient to downregulate p_r. Given that our stimulation protocol evokes spikes in both pre- and postsynaptic cells, these data also indicate that action potential firing and back-propagation alone cannot account for the observed decrease in p_r.

Local Homeostasis Underlies p_r Variability

What might give rise to the observed heterogeneity of p_r? This could be explained if homeostatic regulation of release probability is implemented locally, where spatially distinct parts of the dendritic tree receiving different inputs experience different activity levels and consequently have synapses with dissimilar p_r. In this case, upon forcing inputs to the dendrite to be uniform across the entire dendritic tree, the variability in p_r should become very small. To test this prediction, we used two different experimental conditions to uniformly modulate input to dendrites (Figure 5A). First, we blocked excitatory and inhibitory postsynaptic receptors for 24 hr, thereby rendering all dendrites silent. Second, we uniformly increased dendritic depolarization by raising the KCl concentration in the culture media while blocking postsynaptic receptors for 24 hr. For each case, we then repeated the p_r measurements at individual synapses between identified cell pairs using whole-cell patch clamp and FM dye imaging. Under both conditions, the variability of release

[Handwritten annotation at top of page: "From the same cell, diff amount of activity on diff branches. If we make it more uniform, Pr is more uniform"]
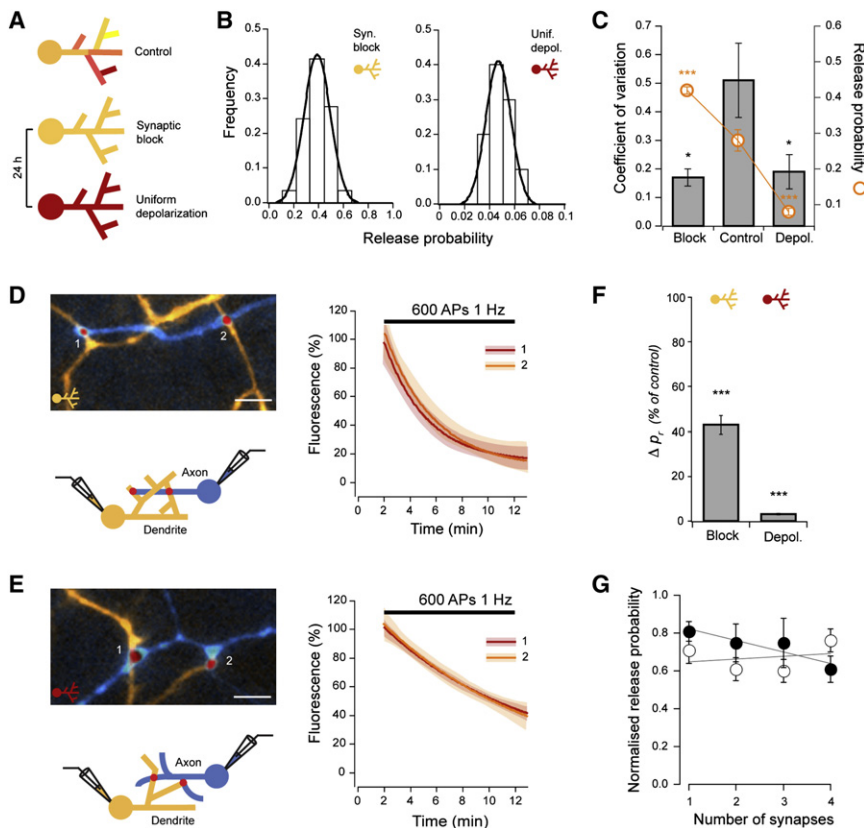

Figure 5. Variability of Release Probability Results from Local Adaptations to Dendritic Activity

(A) Experimental scheme. Inputs to the dendrite were made uniform pharmacologically by treating cultures for 24 hr under "synaptic block" (CNQX, APV, bicuculline) or "uniform depolarization" (CNQX, APV, bicuculline, 20 mM KCl). Release probability was measured by the FM dye destaining rate in paired recordings, as in Figures 1 and 2.

(B) Frequency histograms for two example connections show opposite changes in p_r for synaptic block (left) versus uniform depolarization (right). Lines are Gaussian fits. Note change in the shape of the distribution compared with Figure 1D.

(C) Data summary showing significant decreases in global p_r CV and homeostatic changes in p_r.

(D and E) Example connections of synapses on different dendrites (left) and respective fits to FM4-64 destaining curves (right) for synaptic block (D) and uniform depolarization (E). Scale bars, 5 μm.

(F) Summary of similarity comparisons for both conditions shows that the mean p_r difference for synapses on different dendrites is significantly reduced after the activity manipulations.

(G) Release probability normalized for each connection plotted against the number of synapses in the dendrite for block (open circles) and uniform depolarization (closed circles). The relationship between p_r and synapse density is lost (see Figure 2D). Lines are linear fits to the data. Error bars are ± SEM.

probability was greatly reduced (CV = 0.17 ± 0.03, p = 0.0087, n = 5 for activity block and CV = 0.19 ± 0.06, p = 0.0303, n = 5 for KCl; Figures 5B and 5C), while p_r changed homeostatically in opposite directions (average median p_r = 0.41 ± 0.01, p < 0.0001 for activity block, p_r = 0.07 ± 0.01, p < 0.0001 for KCl; Figures 5B and 5C). Moreover, in accordance with reduced p_r variability, the average absolute p_r difference between all synapses in a connection decreased to 0.12 ± 0.01 for block and 0.03 ± 0.01 for KCl (significantly different from control, p < 0.0001 and p < 0.0001, respectively).

We then repeated the branch-specific spatial analysis of p_r. Given that under these conditions there was a marked decrease in the standard deviation of the p_r distribution, to allow comparisons to control conditions we calculated mean p_r differences as before but then expressed them as a fraction of the control population SD. Consistent with the overall increase in release probability uniformity, mean p_r differences between synapses belonging to different dendritic branches decreased to 43% ± 4% of control for block and to 3% ± 0.4% of control for KCl (p < 0.0001 and p < 0.0001, respectively) and were not significantly different from p_r differences between synapses in the same dendritic branch (p = 0.2660 for block and p = 0.1314 for KCl; see Figures 5D–5F). Furthermore, the relationship between p_r and the number of synapses made on the dendrite was lost (R = −0.03, p = 0.8746 and R = −0.45, p = 0.0804, respectively; Figure 5G). The same increase in similarity was found for recycling pool sizes (Figure S4). The heterogeneity of p_r, therefore, is a consequence of nonuniformity of dendritic activity.

To directly monitor local modulation of p_r, we carried out experiments where we increased synaptic activity to induce homeostatic downregulation of p_r, but restricted stimulation to a subset of synapses in a dendritic branch (Figures 6A and 6B). We then measured p_r by labeling all synapses with FM dye (30 APs, 1 Hz; Figures 6C and 6D). After 2 hr of localized stimulation, release probability of the stimulated synapses was 41% ± 4% lower when compared to unstimulated synaptic neighbors (p < 0.0001), and this effect was blocked by CNQX and APV (p = 0.1872; Figures 6D and 6E). Altogether, these results indicate that the homeostatic control of p_r is implemented locally.

Our spatial analysis of p_r shows that a high degree of p_r similarity in individual dendritic branches occurs only if synapses come from the same presynaptic cell. This implies that p_r homeostasis is triggered by the increased level of postsynaptic activity that is coincident with presynaptic activation. In this case, synapses in a dendrite that belong to the same axon are activated synchronously, and they would adapt to similar levels of dendritic depolarization. On the other hand, synapses from different inputs that are likely to be active asynchronously would produce different depolarization levels, and consequently they would generate different p_r adaptations. To provide experimental support for this hypothesis, we used DIC and FM dye images to trace the axons of synapses analyzed in our local activity manipulation experiments (Figure S6). We found that, in all cases, synapses from different presynaptic cells were found in the stimulated area (Figure 6F, top half) and that, after stimulation, the CV of release probability was significantly reduced to the level of
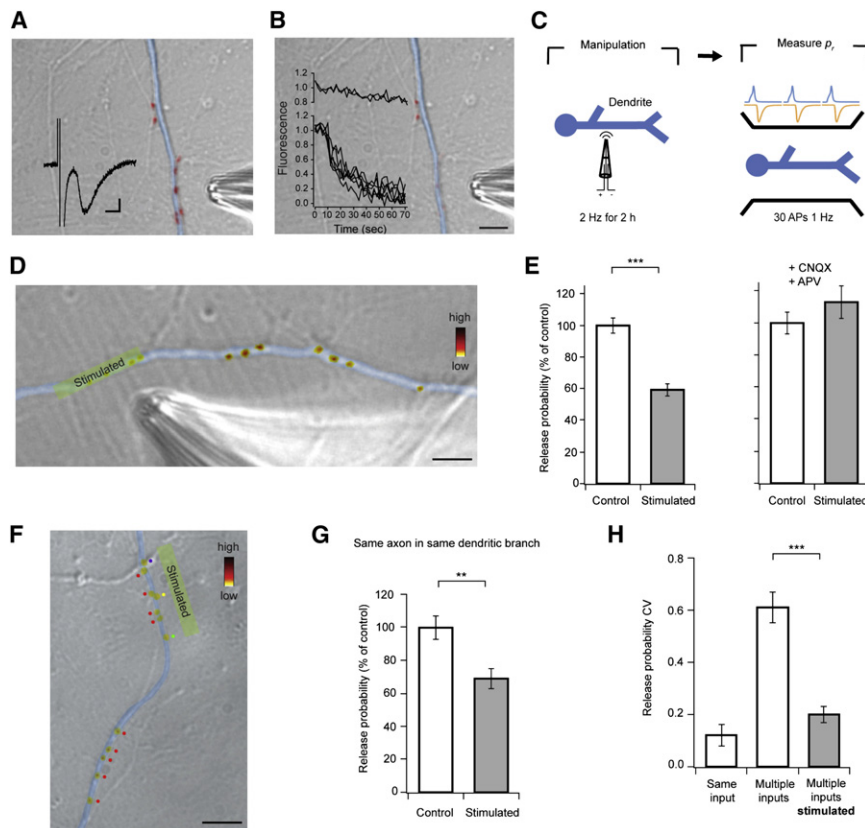
Figure 6. Local Stimulation Decreases Release Probability Selectively

(A and B) Theta-glass pipette stimulation produces a localized synaptic response. (A) Synapses were labeled with FM dye (red), and a whole-cell recording was established. An EPSC (inset trace) was evoked by positioning the stimulating pipette in front of a group of synapses on the dendrite of the recorded cell (colored blue for clarity), confirming successful synaptic stimulation. Scale bars, 2 ms, 10 pA. (B) The same synapses were stimulated by 1200 APs at 20 Hz, and FM dye fluorescence was monitored. Inset graph shows that only the group of synapses directly in front of the pipette lost FM dye fluorescence, indicating high spatial selectivity of the stimulus. Scale bar, 5 μm.

(C) Local stimulation was used to increase synaptic activity in a restricted part of a dendritic branch, and p_r was estimated subsequently by loading synapses with FM dye.

(D) Example DIC image of a dendritic branch with a group of synapses, which were stimulated for 2 hr, with superimposed pseudocolored FM4-64 puncta. Fluorescence intensity represents p_r. Scale bar, 5 μm.

(E) Data summary showing that p_r decreases only in stimulated synapses and that this effect is abolished by synaptic blockers.

(F) Another example image of the same experiment shown in (D), where synapses of interest have been categorized according to the axon they belong to (color dots, see Figure S6 for details on axon tracing procedure). Scale bar, 10 μm.

(G) Data summary showing that local stimulation selectively decreases p_r even if synapses on the dendritic branch belong to the same presynaptic input.

(H) Summary data demonstrating that p_r of synapses from different inputs becomes similar after stimulation. Error bars are ± SEM.

synapses from the same input onto a single dendritic branch (p < 0.0001; Figure 6H). This shows that if two inputs from different presynaptic cells are forced to release synchronously, they acquire similar release probabilities. In some cases, synapses from the same axon were found both in the stimulated and non-stimulated area of the same dendritic branch (Figure 6F, bottom half). Only the stimulated group showed a decrease in p_r (p = 0.0038; Figure 6G), strongly supporting the argument that the p_r similarity found for synapses from the same input onto the same branch results from synchrony of their activation. Taken together, these observations suggest that release probability is downregulated by a coincidence detection mechanism that requires neurotransmitter release and dendritic depolarization.

DISCUSSION

In this study, we combined fluorescence imaging and electrophysiological and ultrastructural methods in dissociated hippocampal cultured neurons to address the determinants of release probability at single synapses. Initially, we considered the spatial organization of p_r. Although the p_r distribution was broad with high CV in pairs of synaptically connected cells, an analysis of

spatial distribution at the level of axonal and dendritic branches showed that synapses made on the same branch of the dendrite had a high degree of similarity. However, when one axon branch contacted different dendritic branches, variability was not significantly different from what might be expected by chance. Because our analysis was always restricted to segments of axons in between two branch points, failures of action potential propagation would not provide a satisfactory explanation for the observation of high p_r variability in the axon. This basic organizational principle of p_r was also supported by two further lines of evidence. First, a spatial relationship similar to that for release probability was established for the total recycling pool size, a known correlate of p_r. Second, a spatial analysis of p_r at EM level also showed dendritic clustering of release probabilities. This suggests that release probability of synapses from a given axon is biased toward acquiring a particular value at individual dendritic branches. Our spatial analysis also revealed an additional salient feature: p_r is inversely correlated with the number of synapses made on the same branch of the dendrite. Since action potential firing in cultured neurons is likely to be random due to a lack of external input, the level of activity of any given part of the dendritic tree should be proportional to the number of

synapses. Thus, the relationship between synapse number and p_r can be viewed as a relationship between activity in the dendrite and release probability. The fact that no such correlation was found for synapses along an axon contacting different dendrites could not be explained by a systematic difference in disposition or density of boutons, since the intersynaptic distance and process length were not different between the two cases. Collectively, these data imply that release probability homeostatically adapts to the level of activity in the dendrite, and since different branches have different mean p_rs, such regulation must be implemented locally. A negative correlation between p_r and synapse density was also found for all synapses along a dendrite, regardless of their origin. However, this correlation was weaker and less steep than for synapses arising from the same input, in line with our argument that the negative feedback regulation we describe is dependent on postsynaptic activation that is coincident with presynaptic activation.

We used paired whole-cell recordings and three different estimates of p_r to explore homeostatic adaptations of release probability. Whereas continuous low-frequency delivery of action potentials to the whole network caused an expected significant decrease in p_r, eliciting action potentials while blocking excitatory synaptic transmission uncoupled pre- and postsynaptic activity and enabled us to investigate the locus of homeostatic plasticity induction. Importantly, stimulating the network in the presence of glutamate receptor blockers represents a different condition to blocking receptors alone. While in the former, evoked neurotransmitter release still occurs, in the latter, the lack of excitatory input abolishes network AP firing. The fact that, in the presence of synaptic blockers, release probability did not decrease despite enhanced axonal activity indicates that a direct action of neurotransmitter on the presynaptic terminal or the average level of depolarization in the presynaptic compartment is not sufficient for homeostatic adaptation of p_r. Rather, it supports the view that neurotransmitter has to depolarize the dendrite for homeostatic mechanisms to be activated.

To address the local nature of the relationship between p_r and dendritic depolarization, we forced spatially uniform depolarization levels along the dendritic tree by either blocking excitatory and inhibitory synaptic input or by increasing the culture medium KCl concentration while blocking postsynaptic receptors. Maintaining these manipulations for 24 hr resulted in a homeostatic change in release probability in which synapses had very similar p_r regardless of their spatial arrangement. Importantly, these manipulations do not represent extremes of membrane potential displacement. Given that, in our system, neurotransmitter release occurs at a rate of ~5 Hz, neurons will spend the majority of time near resting potential. Completely blocking synaptic activity will thus only eliminate the small membrane depolarizations brought about by single or miniature EPSPs, leaving the cell permanently at resting potential. This is clearly a very mild change to the membrane potential, well below changes brought about by inhibition, for example. The KCl manipulation depolarizes the soma by ~15 mV, as measured by whole-cell recording, which, while being stronger than activity block, is well within the limits of physiological relevance. Therefore, the type of p_r regulation we observe is very sensitive to small changes in postsynaptic membrane potential, and the resulting similarity of p_r across synapses

does not represent the consequence of driving synaptic strength to the end of the dynamic range by extreme changes in membrane potential. Furthermore, the finding that under these conditions CV and similarity values for synapses in the same dendrite are the same as in control suggests that the changes elicited by the manipulations are within physiological range and are not taking the system to artifactual limits.

The observed loss of release probability variability upon spatially uniform manipulations of the postsynaptic membrane potential strongly links the p_r heterogeneity with the nonuniformity in inputs to the dendritic tree, thus providing additional support to the idea that the homeostatic response of release probability is implemented at a local level. Furthermore, under these conditions, the inverse relationship between release probability and the number of synapses on the same branch of the dendrite is lost. This is presumably because postsynaptic receptor blockers prevent each synapse from having an impact on dendritic activity, and each individual synapse will adapt to the same average membrane potential. Therefore, in order for a relation between synapse number and p_r to be established, the difference in the number of synapses has to be converted into a difference in local dendritic activity. Importantly, the local regulation of release probability was further confirmed by selectively stimulating a small group of synapses for 2 hr, which produced a compensatory decrease in p_r that was confined to the stimulated area, as was the corresponding increase in similarity.

One possible explanation for the observation of spatial p_r segregation is a developmental one. Given that p_r is developmentally regulated, being initially high and decreasing with maturation (Reyes and Sakmann, 1999; Chavis and Westbrook, 2001), synapses of the same age are expected to have similar release probabilities. In such a case, spatial segregation would reflect developmental age, where synapses in the same branch have been formed at the same time. Although efforts were made to ensure the overall maturity of our cultures (Figure S7), we cannot exclude that different synapses are at different stages of maturation and that this contributes to the observed spatial distribution. However, the inverse correlation between the number of synapses on the dendrite and p_r, and the changes in p_r and its variability imposed by different activity manipulations, highlight the link between postsynaptic activity and release probability and indicate that developmental maturity is not the main variable determining p_r in our system.

A recent study in L2/3 cortical cells has suggested that synapses onto the same postsynaptic target adopt the same p_r, regardless of their position in the dendritic tree. In their study they estimated an overall CV of ~0.20 (Koester and Johnston, 2005). Despite the apparent contradiction with our results, their finding can actually be readily explained by the model of p_r regulation we propose. Assuming there is no systematic bias in the distribution of synapses in vivo, the high and uniform density of synaptic contacts along a given branch will produce, on average, the same activity level. Synapses from a single axon will therefore operate on a similar dendritic activity background irrespective of their location in the dendritic tree, and our model predicts that they will adapt to a release probability representing this background and the depolarization caused by their activation. Given that such synapses share the same presynaptic cell, their

activation rate will be the same and therefore would be expected to develop similar release probabilities. We also believe that our model can fully account for the wide p_r variability observed in autaptic synapses. Given that pure autaptic cultures are isolated from any other inputs, they seldom fire action potentials spontaneously, and thus synaptic activity is restricted to spontaneous neurotransmitter release occurring stochastically in space and time. Given this scenario, and in view of our suggestion that p_r modulation is restricted to activated synapses, the reported variability in autapses is to be expected.

Previous studies have reported homeostatic regulation of p_r in response to inactivity (Murthy et al., 2001; Bacci et al., 2001; Burrone et al., 2002; Thiagarajan et al., 2005; Wierenga et al., 2006), and this is thought to maintain stability in the network while permitting efficient Hebbian learning (Burrone and Murthy, 2003). Likewise, we suggest here that homeostatic setting of basal release probability at individual synapses ensures that each synapse is optimally placed to undergo changes such as those observed in short- and long-term plasticity (Stevens and Wang, 1994). To provide a theoretical basis for this, we simulated a CA1 pyramidal cell receiving a variable number of excitatory synaptic inputs stimulated synchronously. Although in our simplified culture system and some types of connections in the intact hippocampus this corresponds to one axon making multiple contacts in one dendrite, in other cases this would be equivalent to synchronous and layered inputs into the dendritic tree. We found that, while synaptic output increased linearly with increases in release probability when one synapse was stimulated, synchronous activation of more than one synapse led to sublinear responses as p_r approached 1, due to a reduction in the driving force and shunting (Figure S8). Therefore, to prevent saturation of synaptic current, synapses match their release probability to the level of activity on the postsynaptic target. Since each dendrite can behave as a different electrotonic compartment (Rabinowitch and Segev, 2006) and is likely to receive different inputs, this mechanism must be implemented locally to be effective. In contrast to more traditional forms of synaptic homeostasis that are thought to represent a cell-wide phenomenon (Turrigiano and Nelson, 2000), theoretical prediction (Rabinowitch and Segev, 2006) and recent experimental evidence also point to a local homeostatic control of synaptic strength (Ju et al., 2004; Liu, 2004; Sutton et al., 2006). Aside from preventing synaptic saturation, such a mechanism could function to match the strength of synaptic input to the degree of excitability of each dendritic compartment (Polsky et al., 2004).

Collectively, our results indicate that individual synapses must monitor activity of their neighbors and continually adjust their release probability. One important issue that remains to be fully characterized is the extent of the spatial spread of this feedback regulation, which will be dependent on the underlying mechanism. Given the branch-specific distribution of release probability and the triggering of p_r homeostasis with increased depolarization, even in the presence of synaptic blockers, we suggest that a dendritic depolarization-dependent release of a feedback substance might be responsible for p_r homeostasis. Since transient synaptic potentials spread very efficiently through short dendritic branches but decay considerably with branching, a depolarization-based p_r regulation would be expected to mainly affect synapses in the same branch of the dendrite. This could be implemented by known retrograde messengers involved in feedback regulation of release probability, such as the ones described for the *Drosophila* neuromuscular junction (Frank et al., 2006; Davis, 2006) and those thought to underlie both the target-cell dependence of p_r and forms of short-term plasticity or LTD (Duguid and Sjöström, 2006). We cannot, however, exclude the possibility that the spatial spread is in the range of a few microns, something that could be mediated by entry of calcium via GluR2-lacking AMPA receptors, for example. Importantly, our model proposes that this form of p_r homeostasis only affects synapses that have released neurotransmitter. This implies that, apart from a retrograde messenger, some form of coincidence detection is also needed, such as activation of pre- or postsynaptic mGluRs by the released glutamate, for example (Conn and Pin, 1997).

The release probability homeostasis model we propose differs from more classic forms of homeostasis (Turrigiano and Nelson, 2000), not only because it appears to be local but also because it seems to act over a different timescale. Although the direction of change is the same as previously described for presynaptic changes, classic homeostasis is thought to occur over hours/days, whereas our 2 hr activity manipulations were sufficient to change release probability. Furthermore, the finding that this mechanism drives p_r heterogeneity in the resting state indicates that this mode of regulation operates with basal, random, spontaneous activity and is not dependent on some sort of threshold or timed activity. We thus propose that this feedback regulation of p_r acts within a very short integration window, being rapidly activated by each single quanta of neurotransmitter released and continuously operating on the background to quickly adapt release probability to the dendritic environment. This type of model is similar to what Frank et al. (2006) found for the *Drosophila* NMJ and is consistent with that described by Sutton et al. (2006) for postsynaptic scaling. In this way, this mechanism is also different from classic Hebbian plasticity, like LTD, for example, where particular stimulus conditions have to be met for such plasticity to develop. It is worth noting that LTD is, in itself, a form of synaptic homeostasis, and it might be that both forms of plasticity are part of one continuum, the major difference between them being the rate at which voltage perturbations of the membrane potential are imposed.

EXPERIMENTAL PROCEDURES

Cell Culture

Hippocampal neurons were obtained from P0–P1 rat pups and plated at low density onto an astrocyte feeder layer and maintained in Neurobasal-based culture media. Cells were used for experiments at 10–15 days in vitro.

Electrophysiology

Paired whole-cell recordings were obtained with pipettes (3–5 MΩ) containing (in mM) 115 KMeSO$_4$, 5 KCl, 4 NaCl, 10 HEPES, 0.5 CaCl$_2$, 10 creatine phosphate, 2 MgATP, 2 Na$_2$ATP, 0.3 Na$_3$GTP, 10 glutamic acid (pH 7.20), and 100 μM Alexa 488 or 500 μM Alexa 350 hydrazide (Molecular Probes). The external solution contained (in mM) 125 NaCl, 5 KCl, 10 D-glucose, 10 HEPES with 2 CaCl$_2$ and 1 MgCl$_2$ unless otherwise stated (pH 7.30). Recordings were made at 34°C ± 1°C in the presence of 10 μM picrotoxin to isolate excitatory currents and discarded if the access resistance was >30 MΩ (not compensated). Data were acquired with a Multiclamp 700B (Axon Instruments),

filtered to 10 kHz and digitized at 50 kHz. APs were elicited in current clamp by injecting 1 ms 0.5–1 nA current pulses and the postsynaptic cell was voltage clamped, usually at −70 mV (corrected for a junction potential of 10 mV). For paired-pulse experiments, interpulse interval was 50 ms and a minimum of 30 sweeps were acquired at 0.1 Hz. For recordings in low Ca^{2+}, the stimulation frequency was 1 Hz and 100–300 traces were obtained. Data were analyzed with Neuromatic software, and only monosynaptic responses were considered (mean latency 1.94 ± 0.15 ms, 20%–80% rise-time 472 ± 30 μs). In low Ca^{2+} conditions, events were considered to be evoked EPSCs if they fell within the time period defined by the averaged evoked EPSC time course. EPSC integral histograms were constructed using small bins and smoothed with a binomial algorithm in Igor Pro 4.06 (WaveMetrics). The position of the peaks was identified by Gaussian fitting (Larkman et al., 1997). For fitting of a compound binomial model, Monte Carlo simulations of quanta release with varying numbers of release sites and p_r distributions with different CVs were performed in Matlab 7.1 (Mathworks), and the distribution that best fitted the data selected.

Imaging

Epifluorescence images were acquired on an inverted Olympus IX71 microscope using a Micromax cooled-CCD camera (Princeton Instruments) driven by Metamorph software (Universal Imaging). Synapses were labeled with FM4-64 by incubating cultures with 10 μM of dye in extracellular solution containing 90 mM KCl, CNQX (20 μM), and APV (50 μM) for 1 min at room temperature. Following this, neurons were rinsed in normal extracellular solution containing FM4-64 for a further minute to allow completion of endocytosis. Cells were then washed in extracellular solution with 0.5 mM Ca^{2+} and 10 mM Mg^{2+} to minimize dye loss from spontaneous release, and Advasep-7 (1 mM, Biotium) was included for the first minute of the washing procedure to assist with FM dye removal from membranes. For experiments in single cells, neurons were filled with Alexa dye via a patch pipette, and FM dye destaining was evoked either by field stimulation in a custom-made chamber or via the patch pipette, as referred in the text. For connected cells, after a paired recording was obtained and neuronal processes were filled with Alexa dye, a region of interest that included FM-labeled puncta that were likely synaptic contact points between the recorded neurons was chosen, and FM dye destaining was monitored by acquiring images every minute at room temperature. During stimulation, CNQX (20 μM) and APV (50 μM) were used to prevent recurrent stimulation of the network. The fluorescence of each FM dye punctum was quantified using custom-written routines in Igor Pro 4.06 (WaveMetrics) and Matlab 7.1 (Mathworks), and p_r was calculated from the estimated recycling pool size and destaining kinetics (Figure S1). For release probability comparisons between synapses, p_r difference was calculated between each synapse and all other synapses in the branch or cell, depending on the experiment, and this value was averaged. Absolute differences were normalized to the p_r SD of each cell. In an initial set of experiments, the maturity of the synapse population under study was assessed by colabeling synapses with FM4-64 and an antibody raised against the extracellular domain of GluR2 (Chemicon, see Figure S5).

Electron Microscopy

Synaptic vesicles were labeled with a fixable form of 10 μM FM1-43 (FM1-43FX, Molecular Probes) and washed as above. Neurons were fixed, and FM dye was photoconverted in the presence of diaminobenzidine (1 mg/ml) before being prepared for electron microscopy as previously described (Darcy et al., 2006). Serial sections of embedded neurons were placed on formvar-coated slot grids and viewed using an electron microscope (Phillips CM10). Images were acquired using a 1392 × 1040 cooled-CCD camera (Roper Scientific). Synapses and neuronal processes were reconstructed using graphics software (Xara Xtreme) to establish the precise spatial arrangement of axons and dendrites. Photoconverted vesicles have a dark lumen and could be readily distinguished from unstained vesicles using previously described methods (Darcy et al., 2006). For consistency with the fluorescence measurements, the ultrastructural measure of p_r difference was restricted to synapses <10 μm apart (the 90% confidence interval of synapse separation found for the fluorescence-based analysis). 3D reconstructions of processes and presynaptic terminals were made using specialist software ("Reconstruct," J. Fiala, available at http://synapses.bu.edu).

Activity Manipulations

For long-term manipulation of activity, cells were placed in a custom-made chamber and stimulated (2 ms, 5 V pulses, 1–2 Hz field stimulation) while maintaining the culture in the incubator. When required, drugs were added to the culture medium (20 μM CNQX, 50 μM APV, 20 μM bicuculline). All data were obtained in parallel on treated and age-matched sister control cultures.

Statistics

To compare data sets, nonparametric tests (Mann-Whitney U test, Wilcoxon rank sum test, or χ^2 test) were used unless otherwise indicated. Tests for normality and comparisons of distributions were made using Kolmogorov-Smirnov tests. Pearson r test or Spearman r test was used for correlation analysis. Monte Carlo simulations were done by random sampling the theoretical distribution fit to the data. Statistical significance was assumed when p < 0.05. In figures, *p < 0.05, **p < 0.01, and ***p < 0.001. Values in text represent mean ± SEM for normally distributed data and median and interquartile range (IQR) for data that did not meet the criteria for normality.

SUPPLEMENTAL DATA

Supplemental Data include eight figures and can be found with this article online at http://www.neuron.org/cgi/content/full/59/3/475/DC1/.

REFERENCES

Atwood, H.L., and Bittner, G.D. (1971). Matching of excitatory and inhibitory inputs to crustacean muscle fibers. J. Neurophysiol. 34, 157–170.

Bacci, A., Coco, S., Pravettoni, E., Schenk, U., Armano, S., Frassoni, C., Verderio, C., De Camilli, P., and Matteoli, M. (2001). Chronic blockade of glutamate receptors enhances presynaptic release and downregulates the interaction between synaptophysin-synaptobrevin-vesicle-associated membrane protein 2. J. Neurosci. 21, 6588–6596.

Bennett, M.R., Jones, P., and Lavidis, N.A. (1986). The probability of quantal secretion along visualized terminal branches at amphibian (Bufo marinus) neuromuscular synapses. J. Physiol. 379, 257–274.

Biró, A.A., Holderith, N.B., and Nusser, Z. (2005). Quantal size is independent of the release probability at hippocampal excitatory synapses. J. Neurosci. 25, 223–232.

Burrone, J., and Murthy, V.N. (2003). Synaptic gain control and homeostasis. Curr. Opin. Neurobiol. 13, 560–567.

Burrone, J., O'Byrne, M., and Murthy, V.N. (2002). Multiple forms of synaptic plasticity triggered by selective suppression of activity in individual neurons. Nature 420, 414–418.

Cooper, R.L., Harrington, C.C., Marin, L., and Atwood, H.L. (1996). Quantal release at visualized terminals of a crayfish motor axon: intraterminal and regional differences. J. Comp. Neurol. 375, 583–600.

Chavis, P., and Westbrook, G. (2001). Integrins mediate functional pre- and postsynaptic maturation at a hippocampal synapse. Nature 411, 317–321.

Conn, P.J., and Pin, J.P. (1997). Pharmacology and functions of metabotropic glutamate receptors. Annu. Rev. Pharmacol. Toxicol. *37*, 205–237.

Darcy, K.J., Staras, K., Collinson, L.M., and Goda, Y. (2006). Constitutive sharing of recycling synaptic vesicles between presynaptic boutons. Nat. Neurosci. *9*, 315–321.

Davis, G.W. (1995). Long-term regulation of short-term plasticity: a postsynaptic influence on presynaptic transmitter release. J. Physiol. (Paris) *89*, 33–41.

Davis, G.W. (2006). Homeostatic control of neural activity: from phenomenology to molecular design. Annu. Rev. Neurosci. *29*, 307–323.

Del Castillo, J., and Katz, B. (1954). Quantal components of the end-plate potential. J. Physiol. *124*, 560–573.

Dobrunz, L.E., and Stevens, C.F. (1997). Heterogeneity of release probability, facilitation, and depletion at central synapses. Neuron *18*, 995–1008.

Duguid, I., and Sjöström, P.J. (2006). Novel presynaptic mechanisms for coincidence detection in synaptic plasticity. Curr. Opin. Neurobiol. *16*, 312–322.

Frank, E. (1973). Matching of facilitation at the neuromuscular junction of the lobster: a possible case for influence of muscle on nerve. J. Physiol. *233*, 635–658.

Frank, C.A., Kennedy, M.J., Goold, C.P., Marek, K.W., and Davis, G.W. (2006). Mechanisms underlying the rapid induction and sustained expression of synaptic homeostasis. Neuron *52*, 663–677.

Granseth, B., Odermatt, B., Royle, S.J., and Lagnado, L. (2006). Clathrin-mediated endocytosis is the dominant mechanism of vesicle retrieval at hippocampal synapses. Neuron *51*, 773–786.

Harata, N., Ryan, T.A., Smith, S.J., Buchanan, J., and Tsien, R.W. (2001). Visualizing recycling synaptic vesicles in hippocampal neurons by FM 1–43 photoconversion. Proc. Natl. Acad. Sci. USA *98*, 12748–12753.

Harris, K.M., and Sultan, P. (1995). Variation in the number, location and size of synaptic vesicles provides an anatomical basis for the nonuniform probability of release at hippocampal CA1 synapses. Neuropharmacology *34*, 1387–1395.

Hessler, N.A., Shirke, A.M., and Malinow, R. (1993). The probability of transmitter release at a mammalian central synapse. Nature *366*, 569–573.

Huang, E.P., and Stevens, C.F. (1997). Estimating the distribution of synaptic reliabilities. J. Neurophysiol. *78*, 2870–2880.

Jack, J.J., Redman, S.J., and Wong, K. (1981). The components of synaptic potentials evoked in cat spinal motoneurones by impulses in single group Ia afferents. J. Physiol. *321*, 65–96.

Ju, W., Morishita, W., Tsui, J., Gaietta, G., Deerinck, T.J., Adams, S.R., Garner, C.C., Tsien, R.Y., Ellisman, M.H., and Malenka, R.C. (2004). Activity-dependent regulation of dendritic synthesis and trafficking of AMPA receptors. Nat. Neurosci. *7*, 244–253.

Katz, P.S., Kirk, M.D., and Govind, C.K. (1993). Facilitation and depression at different branches of the same motor axon: evidence for presynaptic differences in release. J. Neurosci. *13*, 3075–3089.

Koerber, H.R., and Mendell, L.M. (1991). Modulation of synaptic transmission at Ia-afferent fiber connections on motoneurons during high-frequency stimulation: role of postsynaptic target. J. Neurophysiol. *65*, 590–597.

Koester, H.J., and Johnston, D. (2005). Target cell-dependent normalization of transmitter release at neocortical synapses. Science *308*, 863–866.

Larkman, A.U., Jack, J.J., and Startford, K.J. (1997). Quantal analysis of excitatory synapes in rat hippocampal CA1 in vitro during low-frequency depression. J. Physiol. *505*, 457–471.

Liu, G. (2004). Local structural balance and functional interaction of excitatory and inhibitory synapses in hippocampal dendrites. Nat. Neurosci. *7*, 373–379.

Maass, W., and Zador, A. (1999). Dynamic stochastic synapses as computational units. Neural Comput. *11*, 903–917.

Mennerick, S., and Zorumski, C.F. (1995). Paired-pulse modulation of fast excitatory synaptic currents in microcultures of rat hippocampal neurons. J. Physiol. *488*, 85–101.

Muller, K.J., and Nicholls, J.G. (1974). Different properties of synapses between a single sensory neurone and two different motor cells in the leech C.N.S. J. Physiol. *238*, 357–369.

Murthy, V.N., Sejnowski, T.J., Stevens, C.F., and Zhu, Y. (1997). Heterogeneous release properties of visualized individual hippocampal synapses. Neuron *18*, 599–612.

Murthy, V.N., Schikorski, T., Stevens, C.F., and Zhu, Y. (2001). Inactivity produces increases in neurotransmitter release and synapse size. Neuron *32*, 673–682.

Polsky, A., Mel, B.W., and Schiller, J. (2004). Computational subunits in thin dendrites of pyramidal cells. Nat. Neurosci. *7*, 621–627.

Rabinowitch, I., and Segev, I. (2006). The interplay between homeostatic synaptic plasticity and functional dendritic compartments. J. Neurophysiol. *96*, 276–283.

Redman, S. (1990). Quantal analysis of synaptic potentials in neurons of the central nervous system. Physiol. Rev. *70*, 165–198.

Redman, S., and Walmsley, B. (1983). Amplitude fluctuations in synaptic potentials evoked in cat spinal motorneurones at identified group Ia synapses. J. Physiol. *343*, 135–145.

Reyes, A., and Sakmann, B. (1999). Developmental switch in the short-term modification of unitary EPSPs evoked in layer 2/3 and layer 5 pyramidal neurons of rat neocortex. J. Neurosci. *19*, 3827–3835.

Reyes, A., Lujan, R., Rozov, A., Burnashev, N., Somogyi, P., and Sakmann, B. (1998). Target-cell-specific facilitation and depression in neocortical circuits. Nat. Neurosci. *1*, 279–285.

Robitaille, R., and Tremblay, J.P. (1987). Non-uniform release at the frog neuromuscular junction: evidence of morphological and physiological plasticity. Brain Res. *434*, 95–116.

Rosenmund, C., Clements, J.D., and Westbrook, G.L. (1993). Nonuniform probability of glutamate release at a hippocampal synapse. Science *262*, 754–757.

Schikorski, T., and Stevens, C.F. (2001). Morphological correlates of functionally defined synaptic vesicle populations. Nat. Neurosci. *4*, 391–395.

Slutsky, I., Sadeghpour, S., Li, B., and Liu, G. (2004). Enhancement of synaptic plasticity through chronically reduced Ca+ flux during uncorrelated activity. Neuron *44*, 835–849.

Sorra, K.E., and Harris, K.M. (1993). Occurrence and three-dimensional structure of multiple synapses between individual radiatum axons and their target pyramidal cell in hippocampal area CA1. J. Neurosci. *13*, 3736–3748.

Stevens, C.F., and Wang, Y. (1994). Changes in reliability of synaptic function as a mechanism for plasticity. Nature *371*, 704–707.

Sutton, M.A., Ito, H.T., Cressy, P., Kempf, C., Woo, J.C., and Schuman, E.M. (2006). Miniature neurotransmission stabilizes synaptic function via tonic suppression of local dendritic protein synthesis. Cell *125*, 785–799.

Thiagarajan, T.C., Lindskog, M., and Tsien, R.W. (2005). Adaptation to inactivity in hippocampal neurons. Neuron *47*, 725–737.

Turrigiano, G.G., and Nelson, S.B. (2000). Hebb and homeostasis in neuronal plasticity. Curr. Opin. Neurobiol. *10*, 358–364.

Walmsley, B., Edwards, F.R., and Tracey, D.J. (1988). Nonuniform release probabilities underlie quantal synaptic transmission at a mammalian excitatory central synapse. J. Neurophysiol. *60*, 889–908.

Wierenga, C.J., Walsh, M.F., and Turrigiano, G.G. (2006). Temporal regulation of the expression locus of homeostatic plasticity. J. Neurophysiol. *96*, 2127–2133.

Wittner, L., Henze, D.A., Zaborszky, L., and Buzsaki, G. (2006). Hippocampal CA3 pyramidal cells selectively innervate aspiny neurons. Eur. J. Neurosci. *24*, 1286–1298.

Zakharenko, S.S., Zablow, L., and Siegelbaum, S.A. (2001). Visualization of changes in presynaptic function during long-term synaptic plasticity. Nat. Neurosci. *4*, 711–717.